Environ. Sci. Technol. 1991, 25, 494–500

Photolysis of Chloroform and Other Organic Molecules in Aqueous TiO_2 Suspensions

C. Kormann, D. W. Bahnemann,† and M. R. Hoffmann*

W. M. Keck Laboratories, California Institute of Technology, Pasadena, California 91125

■ The photocatalytic degradation of chloroform has been investigated in aqueous suspensions of TiO_2 over the wavelength range of 310–380 nm. A detailed reaction mechanism has been proposed in which the rate-determining step is the reaction of surface-bound •OH with adsorbed $CHCl_3$. A pH-stat titration technique was developed for the measurement of the rates of degradation of chlorinated hydrocarbons. The quantum efficiency (Φ = 0.56 at λ = 330 nm) of the degradation of $CHCl_3$ was found to be inversely proportional to the square root of the incident light intensity. This relationship can be explained in terms of a direct competition between a second-order recombination of surface-bound •OH and the rate-determining reaction of surface-bound •OH with $CHCl_3$. The rates of degradation of several electron donors have been correlated with their computed surface speciation. The results of this study show that the adsorption of electron donors and acceptors to the TiO_2 surface plays a more important role in determining the rate of the photocatalytic reactions than the effect of pH-dependent Fermi-level shifts.

Introduction

The elimination of toxic chemicals such as halogenated aliphatic and aromatic hydrocarbons from wastewater, soil leachates, and groundwater is presently of great concern. In recent years attention has been directed toward the photocatalytic degradation of organic and inorganic molecules in heterogeneous suspensions of metal oxide semiconductors such as TiO_2 and ZnO (*1–6*). When these semiconductors are illuminated with light of wavelength $\lambda \leq 380$ nm, excited-state electron and hole pairs are produced, which are capable of initiating a wide variety of chemical reactions. Pruden and Ollis (*2*) have shown that chloroform is degraded readily in illuminated suspensions of TiO_2 according to the following stoichiometry:

$$2CHCl_3 + 2H_2O + O_2 \xrightarrow[TiO_2]{h\nu} 2CO_2 + 6HCl \quad (1)$$

In the present work we examine this photochemical reaction in greater detail. The rate of photodegradation of chloroform and several other organic molecules is studied as function of $[CHCl_3]$, pH, $[O_2]$, light intensity, and the presence of charged and neutral solutes. The effect of inhibitors on the rate of chloroform degradation is also studied, and the rate of several photocatalytic reactions is correlated with the calculated surface speciation as determined by a surface chemistry code, SURFEQL (*7, 8*).

Experimental Procedures

Chemicals and solvents were of reagent grade and used without further purification. The water employed in all preparations was purified by a Milli-Q/RO system (Millipore) resulting in a resistivity of $\rho > 18$ MΩ cm. Chloroform (Baker Analyzed, Photorex grade) was extracted with a 10-fold excess of water at least three times before use. A saturated $CHCl_3$ solution ($[CHCl_3]_{aq}$ = 62 mM) was prepared by stirring an excess of chloroform in water at room temperature. Saturation was achieved in <30 min as determined by GC. More dilute solutions were obtained by mixing a saturated stock solution with water. Suspensions of TiO_2 powder (P25, Degussa Corp.) in water were dispersed by simultaneous sonication and shaking for 1 min in an ultrasonic cleaning bath (Branson 5200).

Illumination was carried out with ozone-free 450-W Xe lamps (PRA and Müller) as described previously by Kormann et al. (*9*). Light was filtered by a 10-cm IR water filter and a heat-reflecting UV cutoff filter (transmission at 300 nm <1%). Single-wavelength illuminations were performed by passing the light from the Müller lamp through a Kratos high-intensity monochromator (250 mm focal length). Actinometry was performed with (*E*)-α-[2,5-dimethyl-3-furyl)ethylidene]-3-isopropylidenesuccinic anhydride (*9*). The light intensity for most experiments ranged from 1×10^{-4} to 3×10^{-4} einstein L^{-1} min^{-1} (UV photons, 300 nm < λ < 380 nm). The air-tight photochemical reactors (volume 120 mL) were equipped with magnetic stirring bars, Cl^- ion-selective electrodes (Orion) (vide infra), and their corresponding reference electrodes. Sample aliquots were withdrawn through a Teflon–rubber septum with a microliter syringe. Temperature was monitored with a precision thermometer inserted into the reactor. The reactor temperature was held constant at 23 ± 1 °C with an air-cooled temperature-control system.

The TiO_2 (P25) particles employed in this study were approximately spherical in shape with an average particle diameter of 30 nm. Given a typical incident light intensity of $\sim 2.5 \times 10^{-4}$ einstein L^{-1} min^{-1}, each particle absorbs a single photon on the average of once every 4 ms.

Chloride measurements were performed in situ using a solid-state Cl^- ion-selective electrode (ISE; Orion Model 94-17) and a double-junction reference electrode (Orion Model 90-02-00) linked to a Radiometer ION83 millivolt meter. Analog output was collected by a DASH8 (Metrabyte) A/D converter attached to an IBM/AT PC. Chloride concentrations in split aliquots were also measured by ion chromatography (Dionex 2020i) and were found to agree with the $[Cl^-]$ determined by the ISE within ±5%.

Organic acids were analyzed by ion-exclusion chromatography as described by Munger et al. (*10*). Low molecular weight alcohols and aldehydes were monitored by direct-injection GC (Hewlett-Packard HP 5880A) with FID detection (3-μL injection volumes). Deactivated silica (3 m) and Carbowax (30 m) GC columns were used and run isothermally at 25 °C with a N_2 carrier gas at 1 mL min^{-1} using split injection (split ratio 1:20).

In addition to chloride measurements, a pH-stat titration technique was developed to determine the rates of degradation of organic molecules via the rate of OH^- consumption. The degradation (oxidation) of a general chlorinated hydrocarbon, $C_xH_yCl_z$, can be described by the following stoichiometry:

$$C_xH_yCl_z + \left(x + \frac{y-z}{4}\right)O_2 \rightarrow xCO_2 + zH^+ + zCl^- + \left(\frac{y-z}{2}\right)H_2O \quad (2)$$

† Present address: Institut für Solarenergieforschung, Sokelantstrasse 5, D-3000 Hannover, BRD.

0013-936X/91/0925-0494$02.50/0

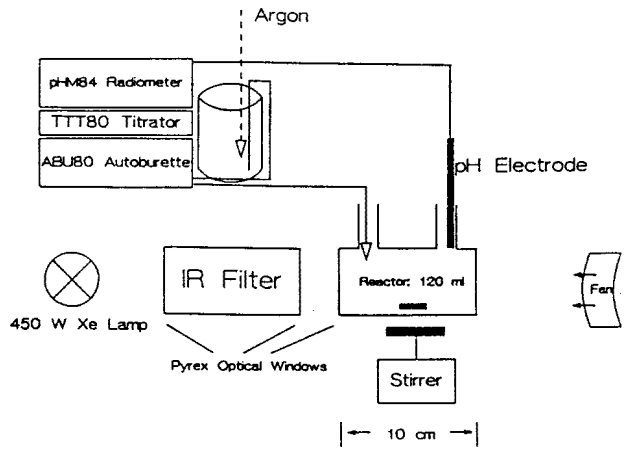

Figure 1. Experimental setup for measuring the rate of degradation of molecules by pH-stat titration. The Radiometer autotitration system consists of a pHM84 pH meter, a TTT80 titrator, and a ABU80 autoburet that is interfaced to a IBM PC-AT computer. A programmable timer on the MBC DASH-8 A/D card was used to count pulses from the ABU80. The titrant solution (0.2 N NaOH) was kept under Ar gas and was calibrated with 0.100 N HCl (Baker Analyzed).

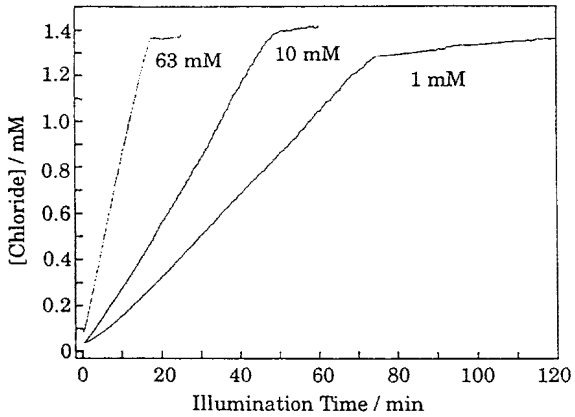

Figure 2. Photocatalytic degradation of $CHCl_3$ shown in terms of the release of Cl^- as function of time for $[TiO_2]$ = 0.5 g L^{-1}, pH 7, $[PO_4^{3-}]_T$ = 10 mM in a sealed reactor (100-mL volume) saturated with air. I_a (310–380 nm) = 2.5 × 10^{-4} einstein L^{-1} min^{-1}.

Since the oxidation of each mole of $C_xH_yCl_z$ leads to the formation of z moles of protons, the autotitration system adds precisely z moles of OH^- to keep the pH constant. A computer code records the derivative of the amount z with respect to time. Since CO_2 will be present as HCO_3^- (pK_{a1} = 6.3) and as CO_3^{2-} (pK_{a2} = 10.3), a correction term is required. In the case of $CHCl_3$, three to five molecules of OH^- are needed for each molecule of $CHCl_3$ oxidized in order to maintain the pH constant (i.e., n(pH) = 3–5).

$$n(\mathrm{pH}) = 3 + \frac{1}{1 + 10^{(6.3-\mathrm{pH})}} + \frac{1}{1 + 10^{(10.3-\mathrm{pH})}} \quad (3)$$

By this approach the rate of $CHCl_3$ degradation is given by

$$-\frac{\mathrm{d}[CHCl_3]}{\mathrm{d}t} = -\frac{\mathrm{d}[OH^-]}{\mathrm{d}t\, n(\mathrm{pH})} \quad (4)$$

Figure 1 illustrates the experimental setup for the pH-stat titration measurements. A comparison of the rates of reaction determined via eq 4 with $\mathrm{d}[Cl^-]/6\ \mathrm{d}t$ measured by use of the chloride ISE showed an agreement of ±2%.

Results

Figure 2 shows the increase in $[Cl^-]$ as a function of time for the photolysis (310 nm ≤ λ ≤ 380 nm) of air-saturated

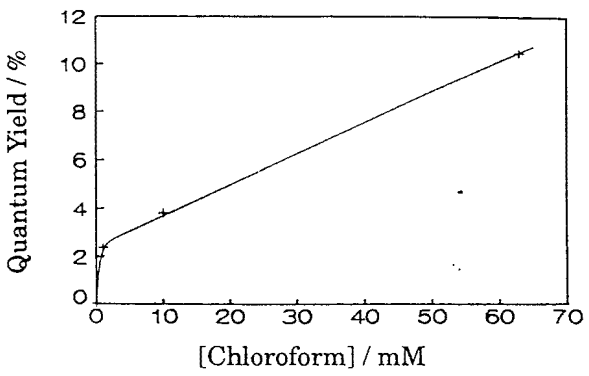

Figure 3. Quantum yield for the photocatalytic degradation of chloroform as function of $[CHCl_3]$. Experimental conditions are the same as given in the caption of Figure 2.

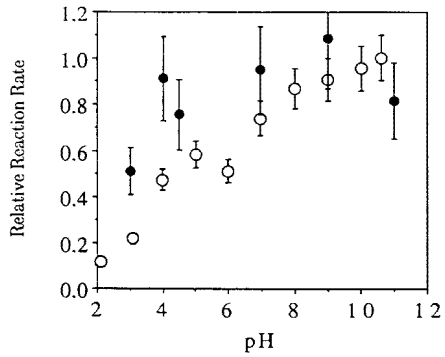

Figure 4. Effect of pH and $[Cl^-]$ on the relative rate of chloroform degradation (expressed in arbitrary units, i.e., normalized rates) where $[TiO_2]$ = 0.5 g L^{-1}, $[CHCl_3]$ = 62 mM, $[O_2]$ = 1.2 mM, and I_a (310–380 nm) = 2.5 × 10^{-4} einstein L^{-1} min^{-1}. ●, no Cl^- present; ○, $[Cl^-]$ = 5 mM, $[CO_3^{2-}]_T$ = 1 mM.

suspensions of TiO_2 in water at three different $CHCl_3$ concentrations (1, 10, 62 mM). The increase in $[Cl^-]$ vs time is linear up to a concentration of ~1.40 ± 0.03 mM (this concentration corresponds to the stoichiometric depletion of O_2), at which point the rate of formation of Cl^- decreases to 1% of the initial rate for $[CHCl_3]_0$ = 62 mM and to 9% of the initial rate for $[CHCl_3]_0$ = 1 mM. The reactor used for these experiments was completely filled (i.e., no headspace) and was sealed tightly from the atmosphere. In the absence of TiO_2, no chloride release was observed.

Figure 3 shows the quantum yield for chloride formation (obtained from the initial slopes of the curves in Figure 2 and the actinometry of the experiment) as a function of the chloroform concentration. The quantum yield (which is proportional to the rate of reaction at constant light intensity) increases sharply between zero and 1 mM chloroform concentration; then a further linear increase is noted over the residual range until $[CHCl_3]$ = 62 mM. In addition, $\mathrm{d}[Cl^-]/\mathrm{d}t$ was found to have a saturation dependence (i.e., Langmurian kinetic dependence) on $[O_2]$. Oxygen concentrations as low as 20 μM were sufficient to yield ~85% of the measured rate of chloroform degradation. The oxygen concentration where the degradation rate reached half of its maximum value was ~5 μM.

In Figure 4 the rate of chloroform degradation is shown as a function of pH for two different cases. In the first case (●), no Cl^- is present at the start of the reaction, while in the second case (○), 5 mM Cl^- and 1 mM CO_3^{2-} are present initially. In each case, $-\mathrm{d}[CHCl_3]/\mathrm{d}t$ is the highest at high pH. In the presence of Cl^-, the pH dependence appears to be more pronounced; whereas, in the absence of Cl^- and CO_2, $-\mathrm{d}[CHCl_3]/\mathrm{d}t$ is approximately the same at pH 4 and 11. In the presence of Cl^- and CO_2 at low pH,

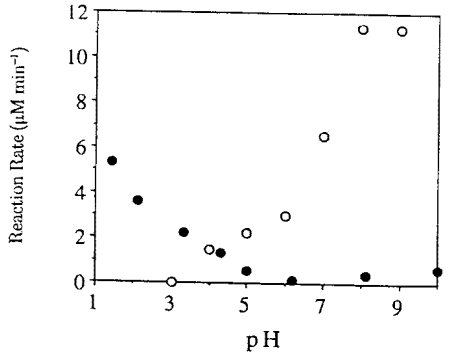

Figure 5. pH dependence of the rate of degradation of trichloroacetate (●) and chloroethylammonium (○) ions where $[CCl_3CO_2^-]_0$ = $[Cl(CH_2)_2NH_2]_0$ = 10 mM, $[TiO_2]$ = 0.5 g L^{-1}, $[O_2]_0$ = 0.25 mM, and I_a (310–380 nm) = 2.5 × 10^{-4} einstein L^{-1} min^{-1}.

the apparent photolysis rate is reduced by approximately 50% of the values observed in the solute-free controls.

Increasing the ionic strength at pH 4 by addition of ClO_4^- did not affect the chloroform degradation rate. However, when Cl^- was used instead to establish the ionic strength, the reaction rate was decreased at pH 4. At pH 10, Cl^- had a negligible effect on the observed rate of chloroform degradation. A change in pH from 4 to 3 resulted in an apparent decrease in the reaction rate by 50% in the presence of 5 mM Cl^-. However, a pH increase from pH 9 to 10 had virtually no effect on the rate of degradation. At pH 4 addition of 5 mM F^- led to the displacement of surface (e.g., ■–TiOH + F^- ⇌ ■–TiF + OH^-) hydroxyl groups without a loss of photocatalytic activity (in fact, an increase in apparent reaction rate by 15% is noted). At pH 7 the addition of up to 10 mM PO_4^{3-}, which is known to be strongly bound to TiO_2 surfaces (*11*), did not affect the rate of chloroform degradation. Whereas at pH 4 1 mM phosphate reduced the reaction rate by 25%.

Various cations, anions, and neutral molecules were found to affect the rate of chloroform degradation at pH 7. Addition of 1 mM Co^{2+} decreased the reaction rate by more than 50%, 0.2 mM Al^{3+} reduced the rate by 70%, and 0.5 mM Zn^{2+} reduced the rate by 60%. The addition of ethanol (e.g., [ethanol] = 2.0 mM) decreased the rate of degradation of chloroform (as measured by the pH-stat technique) by more than 50%. Alcohols and aldehydes were degraded rapidly when they were illuminated in the presence of an air-saturated suspension of TiO_2. The relative order of photodegradation of 200 μM solutions was acetaldehyde ($\tau_{1/2} \simeq 70$ s), 2-propanol ($\tau_{1/2} \simeq 100$ s) > ethanol ($\tau_{1/2} \simeq 160$ s) > methanol ($\tau_{1/2} \simeq 400$ s).

Figure 5 shows the initial rates of degradation of trichloroacetate and of chloroethylammonium ion (each at 10 mM initial concentrations) as a function of pH. The rate of degradation of trichloroacetate is the highest at low pH, while it approaches zero above pH 6. On the other hand, the rate of degradation of chloroethylammonium ion is near zero at pH 3 and increases until it reaches a maximum at pH 8. Only a negligible production of acidity is observed when a solution (10 mM) of chloroethylammonium hydrochloride is illuminated in the absence of TiO_2 at pH 7.7.

Figure 6 shows that the rate of chloroform degradation is a nonlinear function of the light intensity. From this plot we see that the quantum yield of the reaction (as given by the derivative of the plot) increases with decreasing light intensity. The dark line is a square root function fitted to the data points: $-d[CHCl_3]/dt = kI^{1/2}$. In a separate experiment with single-wavelength irradiation at low intensity ($I_{330\,nm}$ = 2.8 × 10^{-6} einstein L^{-1} min^{-1}), a quantum

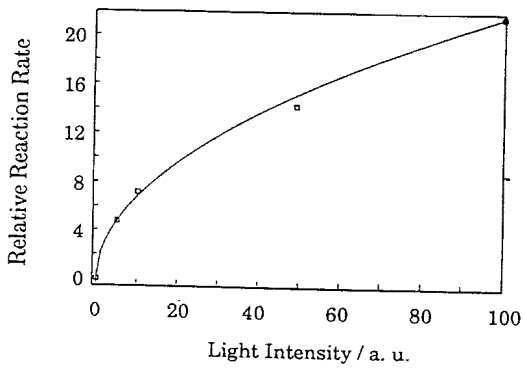

Figure 6. Effect of light intensity (au ≡ arbitrary units, where 100% = 3.0 × 10^{-4} einstein L^{-1} min^{-1}) on rate of chloroform degradation (arbitrary units, i.e., scaled) for $[CHCl_3]_0$ = 63 mM, $[TiO_2]$ = 0.5 g L^{-1}, pH 7.2, $[PO_4^{3-}]_T$ = 10 mM, $[O_2]_0$ = 0.25 mM, reactor volume 120 mL. Illumination with white light of 450-W Xe lamp and light attenuation achieved with neutral-density filters (Oriel no. 5067 5070). (□) experimental data points; (—) square root fit (eq 28).

yield of Φ = 0.56 (measured in terms of $CHCl_3$ degradation) was determined.

Discussion

The overall photocatalytic degradation of chloroform in an oxic suspension of TiO_2 has been shown by Pruden and Ollis (*2*) to have the stoichiometry given in eq 1. A mechanism that is consistent with our experimental observations and the results of Pruden and Ollis is proposed below. The reaction is initiated by the photoexcitation of TiO_2 particles, which leads to the formation of electron–hole pairs:

$$TiO_2 \xrightarrow{h\nu} TiO_2(e_{cb}^- + h_{vb}^+) \quad (5)$$

In the absence of electron donors and acceptors on or near the surface of the excited particle relaxation occurs within a few nanoseconds:

$$TiO_2(e_{cb}^- + h_{vb}^+) \rightarrow TiO_2 + \text{heat} \quad (6)$$

Photogenerated conduction band electrons, e_{cb}^-, can be transferred to an acceptor molecule A at the surface:

$$e_{cb}^- + A \rightarrow A^{\bullet -} \quad (7)$$

Suitable electron acceptors in our system are O_2, $HO_2^\bullet$, H_2O_2, and intermediates from the degradation of chloroform such as $CCl_3O_2^\bullet$.

Likewise, valence band holes, h_{vb}^+, can be filled by suitable electron donors D:

$$h_{vb}^+ + D \rightarrow D^{\bullet +} \quad (8)$$

Potential electron donors in the irradiated $CHCl_3$–TiO_2–O_2 system are H_2O, $CHCl_3$, $HO_2^\bullet$, H_2O_2, Cl^-, OH^-, HCO_3^- and surface hydroxyl groups (e.g., ■–TiOH).

Based on our experimental observations and those of Pruden and Ollis (*2*) we represent the heterogeneous rate of photodegradation of chloroform empirically in terms a second-order kinetic expression:

$$-\frac{d[CHCl_3]}{dt} = k[O_2]_{surf}[CHCl_3]_{surf} \quad (9)$$

where k is an apparent second-order heterogeneous reaction rate constant, $[O_2]_{surf}$ is the concentration of oxygen, and $[CHCl_3]_{surf}$ is the concentration of chloroform adsorbed on the TiO_2 surface. These concentrations can be expressed in terms of the fraction of surface sites occupied by O_2 and $CHCl_3$, respectively. Ollis and co-workers have shown that the extent of adsorption of several chlorinated hydrocarbons can be satisfactorily described in terms of

a Langmuir adsorption isotherm for concentrations $<10^{-3}$ M (*1*). While we are able to confirm their results at low concentrations, we find it necessary to use a two-site Langmuirian model to express the observed rate of reaction for chloroform concentrations up to 62 mM. χ_{CHCl_3}, the fraction of total surface sites occupied by $CHCl_3$, is expressed as follows:

$$\chi_{CHCl_3} = \frac{X_1K_1[CHCl_3]}{1 + K_1[CHCl_3]} + \frac{X_2K_2[CHCl_3]}{1 + K_2[CHCl_3]} \quad (10)$$

where X_1 and X_2 are the fractions of surface sites 1 and 2, respectively, and K_1 and K_2 are the apparent binding constants for adsorption of $CHCl_3$ at surface sites 1 and 2. Thus, $[CHCl_3]_{surf} = \chi_{CHCl_3}[CHCl_3]$. A similar relationship has been used previously to describe the photocatalytic activity of α-Fe_2O_3 particles with S(IV) as an electron donor (*12*). Given our experimental results, we find that $X_1 = 0.02$, $X_2 = 0.98$, $K_1 = 10^4$ M^{-1} and $K_2 = 1$ M^{-1}. The solid line in Figure 3 corresponds to a fit of eq 10 with these values. At low concentrations adsorption is dominated by the tight binding site (X_1), while at higher concentrations (e.g., $[CHCl_3] = 62$ mM) ~75% of the observed rate of reaction is attributed to the loosely binding site (X_2).

The effect of oxygen (data not shown) on the observed reaction rate is described in terms of a simple Langmuir adsorption isotherm as follows:

$$\chi_{O_2} = \frac{K_o[O_2]}{1 + K_o[O_2]} \quad (11)$$

where χ_{O_2} is the fraction of total surface sites occupied by O_2 ($[O_2]_{surf} = \chi_{O_2}[O_2]$ and K_o is the surface binding constant for O_2 on TiO_2. K_o was found to be $13 \pm 7 \times 10^4$ M^{-1}.

The observation that $\Phi \propto I$ suggests a nonlinear mechanism for the photooxidation of chloroform involving the photoproduction of $^{\bullet}OH$. Similar observations have been made by Harvey and Rudman (*13*) in their study of the photocatalytic oxidation of I^-. In our case, we assume that e_{cb}^- is efficiently scavanged by O_2 or by an alternative electron acceptor (e.g., H_2O_2) while h_{vb}^+ has a slightly longer lifetime with respect to electron transfer (i.e., fast recombination is no longer possible). During this longer lifetime, the holes from the bulk solid phase are scavenged by the hydroxylated surface of TiO_2 (*14*) as follows:

$$h_{vb}^+ + OH_{surf}^- \rightarrow {}^{\bullet}OH_{surf} \quad (12)$$

or

$$\blacksquare\text{–TiOH} + h_{vb}^+ \rightarrow \blacksquare\text{–Ti}^+\text{–}{}^{\bullet}OH$$

In turn, the surface-bound hydroxyl radicals ($^{\bullet}OH_{surf}$) are the actual oxidizing agents for chloroform. $^{\bullet}OH$ radical attack is initiated via the abstraction of a hydrogen atom from the surface-bound chloroform as follows:

$$^{\bullet}OH_{surf} + CHCl_{3surf} \xrightarrow{k_r} {}^{\bullet}CCl_{3surf} + H_2O \quad (13)$$

The subsequent steps in the proposed overall mechanism leading to Cl^- production are given in Table I. The rate constant, k_r, for the H atom abstraction by $^{\bullet}OH_{surf}$ can be estimated to be comparable to the corresponding value for the reaction of $^{\bullet}OH$ with chloroform in homogeneous solution ($k = 10^7$ M^{-1} s^{-1}) (*15*). In the overall mechanism (Table I), the active oxidant, $^{\bullet}OH_{surf}$, has an additional loss pathway involving its self-reaction:

$$2{}^{\bullet}OH_{surf} \xrightarrow{k_2} H_2O_{2surf} \quad (14)$$

Salvador and Decker (*16*) have also proposed this recombination as a loss pathway for $^{\bullet}OH_{surf}$ in illuminated TiO_2 suspensions.

Table I. Proposed Mechanism for $CHCl_3$ Degradation

$h_{vb}^+ + OH_{surf}^- \rightarrow {}^{\bullet}OH_{surf}$
$e_{cb}^- + O_{2surf} \xrightarrow{H^+} O_{2surf}^-$
$O_{2surf}^{\bullet-} + H^+ \rightleftharpoons HO_2^{\bullet}$
$^{\bullet}OH_{surf} + CHCl_{3surf} \rightarrow CCl_{3surf}^{\bullet} + H_2O_{surf}$
$CCl_{3surf}^{\bullet} \rightleftharpoons CCl_3^{\bullet}$
$CCl_3^{\bullet} + O_2 \rightarrow CCl_3O_2^{\bullet}$
$2CCl_3O_2^{\bullet} \rightarrow 2CCl_3O^{\bullet} + O_2$
$CCl_3O^{\bullet} + HO_2^{\bullet} \rightarrow CCl_3OH + O_2$
$CCl_3OH \rightarrow Cl_2C{=}O + H^+ + Cl^-$
$Cl_2C{=}O + H_2O \rightarrow CO_2 + 2H^+ + 2Cl^-$

Assuming a photostationary state for $^{\bullet}OH_{surf}$, we can write the following steady-state equation:

$$\frac{d[^{\bullet}OH_{surf}]}{dt} = I_a\Phi_{^{\bullet}OH} - k_r[^{\bullet}OH_{surf}][CHCl_{3surf}] - k_2[^{\bullet}OH_{surf}]^2 = 0 \quad (15)$$

where $\Phi_{^{\bullet}OH}$ is the quantum yield for $^{\bullet}OH_{surf}$ production and I_a is the intensity of absorbed light. If we assume that $\Phi_{^{\bullet}OH} \approx 1$, then we can express the quantum yield for chloroform degradation in terms of k_r and k_2 as follows:

$$\Phi_r = \frac{k_r[^{\bullet}OH_{surf}][CHCl_{3surf}]}{k_r[^{\bullet}OH_{surf}][CHCl_{3surf}] + k_2[^{\bullet}OH_{surf}]^2} \quad (16)$$

We can consider two limiting cases. In the first case, we can neglect the second-order term under conditions of low light intensity

$$k_r[^{\bullet}OH_{surf}][CHCl_{3surf}] \gg k_2[^{\bullet}OH_{surf}]^2 \quad (17)$$

and see that Φ_r approaches unity. In the second case, under conditions of high light intensity we can neglect the $k_r[^{\bullet}OH_{surf}][CHCl_{3surf}]$ term in eq 15 and obtain

$$I_a - k_2[^{\bullet}OH_{surf}]^2 = 0 \quad (18)$$

Thus, under these conditions the concentration of $^{\bullet}OH_{surf}$ is controlled by its second-order recombination to give

$$[^{\bullet}OH_{surf}] = (I_a/k_2)^{1/2} \quad (19)$$

In addition we see that Φ_r decreases with increasing light intensity as follows:

$$\Phi_r = \frac{k_r[^{\bullet}OH_{surf}][CHCl_{3surf}]}{I_a} = \frac{k_r[CHCl_{3surf}]}{(k_2I_a)^{1/2}} \quad (20)$$

From a single-wavelength illumination experiment at 330 nm we obtained $\Phi_r = 0.56$ ($I_a = 4.64 \times 10^{-8}$ einstein L^{-1} s^{-1} and $[CHCl_3]_0 = 62$ μM). Using eq 10 and the associated constants we obtain a value of $k_r/(k_2)^{1/2}$ of 2×10^{-3} $M^{-1/2}$ $s^{-1/2}$. From this ratio we see that k_r is small compared to k_2.

With the experimental results presented above we have shown that a variety of solutes affect the rate of chloroform degradation depending on the specific nature of the solute and the pH of the suspension. Simple anions such as Cl^- and HCO_3^- decrease the photoefficiency of the catalyst at low pH where they can be adsorbed to the positively charged TiO_2 particle surface ($pH_{zpc} = 6.25$ for P25 TiO_2). However, the same anions have a negligible affect on the measured photoefficiency at high pH since their adsorption to reactive surface sites is prevented by electrostatic repulsion from the negatively charged TiO_2 particles. The adsorption of the negatively charged anions is stronger the higher the positive surface charge. Thus, we saw a significant reduction in reaction rate as the pH was lowered from 4 to 3 in the presence of Cl^-.

Inhibition of $CHCl_3$ photooxidation by cations, anions, and neutral molecules results from the competition for reactive surface sites and from the competition for reactive intermediates such as $^{\bullet}OH_{surf}$. While some molecules such as Cl^-, HCO_3^-, and C_2H_5OH react readily with $^{\bullet}OH$, other molecules such as F^- and ClO_4^- are essentially unreactive and thus have no effect on the net oxidation rate of $CHCl_3$.

We can summarize the effects of competitive solutes (i.e., quenchers) on the oxidation of $CHCl_3$ by considering a mechanism involving eqs 13 and 21

$$^{\bullet}OH_{surf} + Q_{surf}{}^{i} \xrightarrow{k_q} \text{products} \qquad (21)$$

The reaction of $^{\bullet}OH_{surf}$ with surface-adsorbed quenchers ($Q_{surf}{}^{i}$) is an inhibition process with a characteristic rate constant of k_q. The reaction of eq 21 effectively competes for $^{\bullet}OH_{surf}$ and reduces its relative rate with $CHCl_{3surf}$. Thus, higher concentrations of quencher molecules present at the particle surface during illumination will result in more extensive inhibition of chloroform degradation.

If we assume that the formation of $^{\bullet}OH_{surf}$ radicals is the rate-determining step, we can represent mathematically the effect of the quencher molecules on the rate of $CHCl_3$ degradation for the photostationary state as follows:

$$\frac{d[^{\bullet}OH_{surf}]}{dt} =$$

$$k_r[^{\bullet}OH_{surf}][CHCl_{3surf}] + [^{\bullet}OH_{surf}]\sum_{i=1}^{n} k_q{}^{i}[Q_{surf}{}^{i}] = 0 \qquad (22)$$

where

$$[^{\bullet}OH_{surf}] = \frac{d[^{\bullet}OH_{surf}]/dt}{k_r[CHCl_{3surf}] + \sum_{i=1}^{n} k_q{}^{i}[Q_{surf}{}^{i}]} \qquad (23)$$

From eq 13 the overall rate of chloroform degradation is given by

$$-\frac{d[CHCl_3]}{dt} = k_r[^{\bullet}OH_{surf}][CHCl_{3surf}] \qquad (24)$$

Substitution of eq 23 into eq 24 yields

$$-\frac{d[CHCl_3]}{dt} = \frac{d[^{\bullet}OH_{surf}]/dt\,[CHCl_{3surf}]}{k_r[CHCl_{3surf}] + \sum_{i=1}^{n} k_1{}^{i}[Q_{surf}{}^{i}]} \qquad (25)$$

or

$$-\frac{d[CHCl_3]}{dt} = \frac{d[^{\bullet}OH_{surf}]/dt}{1 + \sum_{i=1}^{n} k_q{}^{i}[Q_{surf}]/k_r[CHCl_{3surf}]} \qquad (26)$$

Taking the double reciprocal of eq 26 we obtain

$$\left(-\frac{d[CHCl_3]}{dt}\right)^{-1} = \left(\frac{d[^{\bullet}OH_{surf}]}{dt}\right)^{-1} + \sum_{i=1}^{n} \frac{k_q{}^{i}[Q_{surf}{}^{i}]}{d[^{\bullet}OH_{surf}]/dt\,k_r[CHCl_{3surf}]} \qquad (27)$$

We can simplify this latter equation to give

$$\nu_{CHCl_3}{}^{-1} = \sum_{i=1}^{n} k[Q_{surf}{}^{i}] + \nu_{OH^{\bullet}}{}^{-1} \qquad (28)$$

where $\nu_{CHCl_3}{}^{-1} = (-d[CHCl_3]/dt)^{-1}$, $\nu_{OH^{\bullet}}{}^{-1} = (d[^{\bullet}OH_{surf}]/dt)^{-1}$, and

$$k = \frac{k_q{}^{i}}{d[^{\bullet}OH_{surf}]/dt\,k_r[CHCl_{3surf}]} \qquad (29)$$

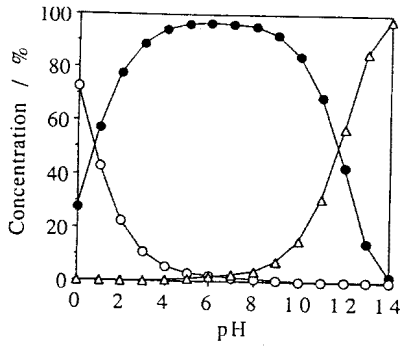

Figure 7. Surface speciation of TiO_2 particles as function of pH. Calculated with the following primary data: $pK_{a1}{}^{s} = 2.4$, $pK_{a2}{}^{s} = 8.0$, $\mu = 0.01$ M, surface exchange capacity 0.46 mol g^{-1}, surface area 50 m^2 g^{-1}, and solids concentration 0.5 g L^{-1}. (●) ■–TiOH; (○) ■–$TiOH_2^+$; (△) ■–TiO^-.

k and $\nu_{OH^{\bullet}}{}^{-1}$ are constants for any given experiment where the chloroform concentration and the light intensity are held constant. In order to obtain the surface concentration [Q_{surf}] of charged quenchers, the electrostatic interaction between the charged surface and the aqueous-phase quenchers has to be calculated.

The nature of the metal oxide surface in aqueous solution has been treated in detail previously (*17*). Surface groups of a metal oxide are amphoteric and the surface acid–base equilibria can be written

$$\blacksquare\text{–}TiOH_2^+ \rightleftharpoons \blacksquare\text{–}TiOH + H^+ \qquad (30)$$

$$\blacksquare\text{–}TiOH \rightleftharpoons \blacksquare\text{–}TiO^- + H^+ \qquad (31)$$

where ■–TiOH represents the "titanol" surface group. $K_{a1}{}^{s}$, $K_{a2}{}^{s}$, and the pH_{zpc} ($pH_{zpc} = (pK_{a1}{}^{s} + pK_{a2}{}^{s})/2 = 6.25$) may be determined by titration and other experimental techniques (*17*, *18*). The microscopic (i.e., apparent) acidity constants in these equations are related with the intrinsic acidity constants via

$$K_{ai}{}^{s} = {}^{int}K_{ai}{}^{s} e^{F\psi_{H^+}/RT} \qquad (32)$$

where ${}^{int}K_{ai}{}^{s}$ is the intrinsic acidity constant (i.e., the acidity constant in a hypothetically chargeless environment), ψ_{H^+} is the effective potential difference between the binding site and the bulk of the solution for H^+, and F, R, and T have their usual definitions. The relationship between the surface charge, σ_o, and the surface potential in a diffuse layer model has been derived previously (*19*).

We utilized the computer code SURFEQL (*7*) to perform surface equilibrium calculations in an attempt to model the surface chemistry of charged substrates relevant to the conditions of this study. SURFEQL has been used successfully to calculate equilibrium distributions of chemical species in a number of cases (*20*, *21*). The set of experimental conditions and surface acidity constants used for the simulations for TiO_2 surface chemistry are as follows: $pK_{a1}{}^{s} = 2.4$ (*22*); $pK_{a2}{}^{s} = 8.0$ (*22*); ionic strength, $\mu = 0.01$ M; surface exchange capacity = 0.46 mol g^{-1} (*23*); surface area = 50 m^2 g^{-1} (*24*); solids concentration of 0.5 g L^{-1}.

Results of these computations are illustrated in Figure 7, which shows the surface speciation obtained in the absence of surface complexation by ligands (i.e., other than water) present in solution. As illustrated in Figure 7, the neutral surface species ■–TiOH is predominent over a broad range of pH. At pH <6 the TiO_2 surface accumulates a net positive charge due to the increasing fraction of total surface sites present as ■–$TiOH_2^+$. At high pH, the surface has a net negative charge due to a significant

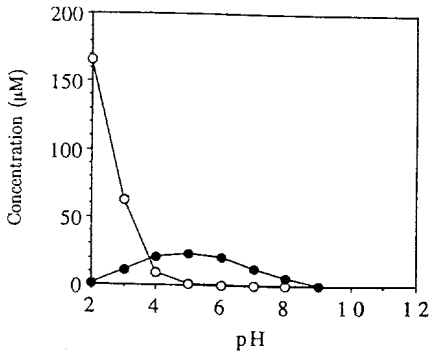

Figure 8. Calculated (SURFEQL) concentrations of ■–$TiCO_3^-$ (●) and ■–TiCl (○) surface complexes as a function of pH. General conditions are the same as in the caption of Figure 7 with $pK_{Cl^-}^s = 5$ and $pK_{CO_3^{2-}}^s = 13$.

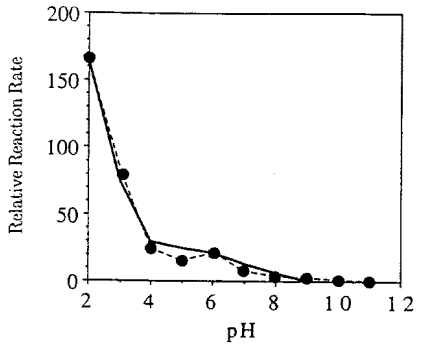

Figure 9. Inhibition of the photocatalytic degradation of chloroform by Cl^- and CO_3^{2-} as a function of pH expressed in arbitrary units (scaled units). Experimental (●) and calculated (—) behavior according to eq 28. Computational conditions as described in Figures 7 and 8.

fraction of total surface sites present as ■–TiO^-.

Ligands such as Cl^-, F^-, CO_3^{2-}, and HPO_4^{2-} are known to form inner-sphere surface complexes (*17*) as follows:

$$\blacksquare\text{–TiOH} + Cl^- + H^+ \overset{K_{Cl^-}^s}{\rightleftharpoons} \blacksquare\text{–TiCl} + H_2O \quad (33)$$

$$\blacksquare\text{–TiOH} + CO_3^{2-} + H^+ \overset{K_{CO_3^{2-}}^s}{\rightleftharpoons} \blacksquare\text{–TiCO}_3^- + H_2O \quad (34)$$

In some cases, surface complex formation constants are available in the literature (*25*). However, values for $K_{Cl^-}^s$ and $K_{CO_3^{2-}}^s$ are not known and thus they will be treated as adjustable parameters our model development. Figure 8 shows the pH-dependent variation of the important surface complexes in the presence of Cl^- and CO_3^{2-}. The formation of ■–TiCl is significant only at low pH, while at pH >6.2 the attachment Cl^- to the surface is negligible. The concentration of ■–$TiCO_3^-$ is highest at pH ≃5. At high pH, electrostatic repulsion makes formation of this complex impossible, while at low pH the concentration of CO_3^{2-} is too low, thus shifting the equilibrium of eq 34 to the left. The specific surface complex formation constants used in Figure 8 were $K_{Cl^-}^s = 10^5$ M^{-1} and $K_{CO_3^{2-}}^s = 10^{13}$ M^{-1}; these constants were obtain by correlation with the corresponding formation constants for the analogous complexes in homogeneous aqueous solution (*17*). A change in the order of magnitude of these constants does not alter the qualitative observation that the attachment of Cl^- occurs to a greater degree at low pH and that the attachment of CO_3^{2-} is at maximum at pH 5.

The surface complex formation constants were optimized such that the observed kinetic inhibition of Cl^- and CO_3^{2-} was matched. Figure 9 shows that a plot of the $\nu_{CHCl_3}^{-1}$ vs pH parallels the concentration of surface-bound inhibitor as a function of pH, as predicted by eq 28. To

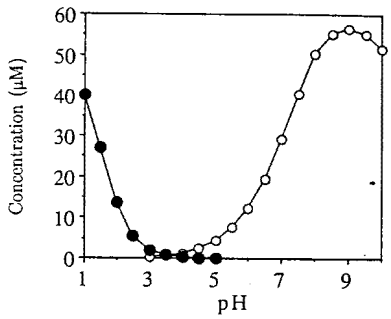

Figure 10. Concentrations of ■–$TiO_2CO_2CCl_3$ (●) and ■–$TiN^+H_2CH_2CH_2Cl$ (○) surface complexes as a function of pH. Computational conditions as given in Figure 7 along with $pK_{TCAc^-}^s = 4$ and $pK_{RNH_2}^s = 9.5$.

generate this plot it was assumed that the two surface-bound inhibitors (Cl^- and HCO_3^-) reacted equally fast with the excited-state TiO_2 particles. This assumption is supported by previous studies that show many oxidizable molecules are photodegraded at rates that vary by less than a factor of 10 (*1*, *4*).

We note that $^{\bullet}OH_{surf}$ may have a reactivity similar to its counterpart ($^{\bullet}OH_{aq}$) in homogeneous aqueous solution. In previous studies (*9*, *26*) we found that glyoxylic and gycolic acid are formed during the photocatalytic degradation of acetate. The appearance of these products may be taken as further proof that the oxidizing species at the surface has the reactivity of $^{\bullet}OH_{surf}$ rather than of h_{cb}^+ since the same reaction products are found when $^{\bullet}OH$ radicals oxidize acetate in homogeneous aqueous solution (*27*).

The enhanced rate of oxidation of cations at high pH (see Figure 5) cannot be explained by a simple shift of the Fermi level of the TiO_2 particles as argued by other investigators (*19*). If such an effect were the dominant influence on the photoactivity of TiO_2 as a function of pH, then we should see the opposite kinetic behavior in which lower rates of degradation should be observed at high pH. Adsorption of the electron donor to the surface of TiO_2 particles appears to play a more important role in the resultant photochemistry than does the shift in the location of the Fermi level. To illustrate this point further, we again assume that the rate of photodegradation is proportional to the concentration of the electron donor at the surface. Using SURFEQL we determined the concentrations of surface complexes as given by the following equilibria (Figure 10):

$$\blacksquare\text{–TiOH} + CCl_3CO_2^- + H^+ \overset{K_{Ac^-}^s}{\rightleftharpoons} \blacksquare\text{–TiO}_2CCl_3 + H_2O \quad (35)$$

$$\blacksquare\text{–TiOH} + ClCH_2CH_2NH_2 + H^+ \overset{K_{RNH_2}^s}{\rightleftharpoons} \blacksquare\text{–TiN}^+H_2(CH_2)_2Cl + H_2O \quad (36)$$

where $K_{Ac^-}^s = 10^4$ M^{-1} and $K_{RNH_2}^s = 10^{9.5}$ M^{-1} (for $CCl_3CO_2^-$ $pK_a = 0.7$ and for chloroethylammonium ion $pK_a = 8$ (*28*)). As shown in Figure 10, the concentration of ■–TiO_2CCl_3 is essentially zero at high pH and increases at pH values less than the pH_{zpc} of TiO_2. Conversely, the formation of ■–$TiN^+H_2(CH_2)_2Cl$ is favored at high pH in a pH domain where the amine is present as $Cl(CH_2)_2NH_3^+$ and the TiO_2 surface has substantial sites present as ■–TiO^-. The surface concentration of ■–$TiN^+H_2(CH_2)_2Cl$ decreases at pH > 9 as the concentration of the protonated amine increases. If we compare the experimental results shown in Figure 5 to the calculated results of Figure 10, we see that the surface complexation model appears to predict the effects of pH and charge on the observed heteroge-

neous photochemical reactivity of charged molecules.

Acknowledgments

We are grateful to Drs. Dieter Gunz and German Mills for their help on this project. We appreciate the generous donation of the P25 TiO_2 by the Degussa Corp.

Registry No. $CHCl_3$, 67-66-3; TiO_2, 13463-67-7.

Literature Cited

(1) Ollis, D. F. *Environ. Sci. Technol.* **1985**, *19*, 480.
(2) Pruden, A. L.; Ollis, D. F. *Environ. Sci. Technol.* **1983**, *17*, 628.
(3) Matthews, R. W. *J. Chem. Soc., Faraday Trans. 1* **1984**, *80*, 457.
(4) Matthews, R. W. *Water Res.* **1986**, *20*, 569.
(5) Matthews, R. W. *J. Phys. Chem.* **1987**, *91*, 3328.
(6) Pelizetti, E.; Borgarello, M.; Minero, C.; Pramauro, E.; Borgarello, E.; Serpone, N. *Chemosphere* **1988**, *17*, 499.
(7) Faughnan, J. *SURFEQL—An Interactive Code for the Calculation of Chemical Equilibria in Aqueous Solution*; W. M. Keck Laboratories, California Institute of Technology: Pasadena, CA, 1981.
(8) Westall, J. C.; Hohl, H. *Adv. Colloid Interface Sci.* **1980**, *12*, 265.
(9) Kormann, C.; Bahnemann, D. W.; Hoffmann, M. R. *Environ. Sci. Technol.* **1988**, *22*, 798.
(10) Munger, J. W.; Collett, J.; Daube, B. C.; Hoffmann, M. R. *Tellus* **1989**, *41B*, 230.
(11) Hadjiivanov, K. I.; Klissurski, D. G.; Davydov, A. A. *J. Catal.* **1989**, *116*, 498.
(12) Faust, B. C.; Hoffmann, M. R. *Environ. Sci. Technol.* **1986**, *20*, 943.
(13) Harvey, P. R.; Rudham *J. Chem. Soc., Faraday Trans. 1* **1988**, *84*, 4181.
(14) Brown, G. T.; Darwent, J. R. *J. Phys. Chem.* **1984**, *88*, 4955.
(15) Farhataziz; Ross, A. B. *NBS Spec. Publ. (U.S.)* **1977**, *3*, 32, NSRDS-DBS 59.
(16) Salvador, P.; Decker, F. *J. Phys. Chem.* **1984**, *88*, 6116.
(17) Stumm, W.; Morgan, J. J. *Aquatic Chemistry*, 2nd ed.; Wiley Interscience: New York 1981; pp 625–640.
(18) Kormann, C.; Bahnemann, D. W.; Hoffmann, M. R. *J. Phys. Chem.* **1988**, *92*, 5196.
(19) Bard, A. J.; Faulkner, L. R. *Electrochemical Methods. Fundamentals and Applications*; Wiley: New York, 1980.
(20) Faust, B. C.; Bahnemann, D. W.; Hoffmann, M. R. *J. Phys. Chem.* **1989**, *93*, 6371.
(21) Davies, S. H. R.; Morgan, J. J. *J. Colloid Interface Sci.* **1989**, *129*, 63.
(22) Wehrli, B. Ph.D. Thesis, ETH No. 8232, Zurich, Switzerland, 1987.
(23) Herrmann, M.; Boehm, H. P. *Z. Anorg. Chem.* **1969**, *73*, 368.
(24) Degussa Corp. *Technical Bulletin Pigments*, 4th ed.; Degussa: Hanau-Wolfgang, FRG, 1984; No. 56.
(25) Dzombak, D. A.; Morel, F. M. M. *Surface Complexation Modeling*; Wiley-Interscience: New York, 1990; pp 393.
(26) Kormann, C.; Bahnemann, D. W.; Hoffmann, M. R. *J. Phys. Chem.* **1987**, *91*, 3789.
(27) Schuchmann, M. N.; Zegota, H.; von Sonntag, C. *Z. Naturforsch.* **1985**, *408*, 215.
(28) Smith, R. M.; Martell, A. E. *Critical Stability Constants*, Vol. 2 *Amines*; Vol. 3 *Other Ligands*; Plenum Press: New York, 1975, 1977.

Received for review September 7, 1990. Accepted October 2, 1990. This research was supported by grants from the U.S. Environmental Protection Agency (R 813326-01-0 and R 815041-01-0).

Sediment Trap Fluxes and Benthic Recycling of Organic Carbon, Polycyclic Aromatic Hydrocarbons, and Polychlorobiphenyl Congeners in Lake Superior

Joel E. Baker,*,† Steven J. Eisenreich,† and Brian J. Eadie‡

Environmental Engineering Sciences, Department of Civil and Mineral Engineering, University of Minnesota, Minneapolis 55455, and Great Lakes Environmental Research Laboratory, NOAA, 2205 Commonwealth Boulevard, Ann Arbor Michigan 48105

■ Sediment trap fluxes of solids, organic carbon, polycyclic aromatic hydrocarbons (PAHs), and polychlorinated biphenyls (PCBs) were measured in Lake Superior in 1984 and 1985. Mass fluxes from surface waters ranged from 0.14 to 1.1 g/m^2-day and increased near the lake floor due to resuspension of surficial sediment and horizontal transport in the benthic nepheloid layer. Organic matter fluxes from surface waters ranged from 60 to 90 mg of C/m^2-day, with ~5% of organic carbon settling from surface waters accumulating in bottom sediments. Concentrations of PCBs and PAHs are enriched 10–100 times on settling particles relative to those on suspended particles. Resultant settling fluxes are 10–100 times greater for several PCB and PAH compounds than net accumulation rates in bottom sediments, indicating the effective and rapid recycling in the benthic region. Biological packaging of organic pollutants into rapidly settling particles is an efficient pathway for the transport of contaminants from surface waters to benthic regions of large lakes.

Introduction

Cycling of many chemical species in natural waters is intimately linked to the production, transport, and loss of particles within the water column. Associations with settling particles control the water column residence times of hydrophobic organic contaminants (HOCs) such as polychlorobiphenyls (*1*) as well as many trace metals (*2–6*). In the long term, burial of contaminants in bottom sediments serves as an important self-purification mechanism in lakes, estuaries, and oceans. On shorter time scales, however, the dynamics of particle formation and transport drive spatial and temporal variations in the water column inventories of particle-associated species. Such fluctuations may increase net contaminant residence times and dampen the water column response to decreased loadings. In this study, we report on the interwoven cycles of particulate matter, organic carbon, and hydrophobic organic contaminants in oligotrophic Lake Superior.

Processes controlling the type and quantity of suspended solids in the water column of the Laurentian Great Lakes include shoreline erosion, resuspension of surficial sediments, primary production, and calcite precipitation (*3*). Each of these sources varies in response to changes in hydrodynamics, weather, and season. In large lakes and in the oceans, degradation of organic particles is very efficient and only a small fraction of primary production is incorporated into sediments (*7–9*).

The chemical composition of particles suspended in the water column also varies spatially and temporally. During

* Address correspondence to this author at the Chesapeake Biological Laboratory, Center for Environmental and Estuarine Studies, The University of Maryland System, Solomons, MD, 20688.
† University of Minnesota.
‡ NOAA.

0013-936X/91/0925-0500$02.50/0